Hindawi Publishing Corporation
Journal of Biomedicine and Biotechnology
Volume 2012, Article ID 828139, 9 pages
doi:10.1155/2012/828139

Research Article

Development of ^{99m}Tc-N4-NIM for Molecular Imaging of Tumor Hypoxia

Mohammad S. Ali,[1] Fan-Lin Kong,[1] Alex Rollo,[1] Richard Mendez,[1] Saady Kohanim,[1] Daniel Lee Smith,[2] and David J. Yang[1]

[1] *Department of Experimental Diagnostic Imaging, The University of Texas MD Anderson Cancer Center, Houston, TX 77030, USA*
[2] *Department of Radiation Physics, The University of Texas MD Anderson Cancer Center, Houston, TX 77030, USA*

Correspondence should be addressed to Mohammad S. Ali, mohammad.ali@mdanderson.org

Received 31 January 2012; Revised 24 March 2012; Accepted 1 April 2012

Academic Editor: Yasuhisa Fujibayashi

The nitro group of 2-nitroimidazole (NIM) enters the tumor cells and is bioreductively activated and fixed in the hypoxia cells. 1,4,8,11-tetraazacyclotetradecane (N4) has shown to be a stable chelator for ^{99m}Tc. The present study was aimed to develop ^{99m}Tc-cyclam-2-nitroimidazole (^{99m}Tc-N4-NIM) for tumor hypoxia imaging. N4-NIM precursor was synthesized by reacting N4-oxalate and 1,3-dibromopropane-NIM, yielded 14% (total synthesis). Cell uptake of ^{99m}Tc-N4-NIM and ^{99m}Tc-N4 was obtained in 13762 rat mammary tumor cells and mesothelioma cells in 6-well plates. Tissue distribution of ^{99m}Tc-N4-NIM was evaluated in breast-tumor-bearing rats at 0.5–4 hrs. Tumor oxygen tension was measured using an oxygen probe. Planar imaging was performed in the tumor-bearing rat and rabbit models. Radiochemical purity of ^{99m}Tc-N4-NIM was >96% by HPLC. Cell uptake of ^{99m}Tc-N4-NIM was higher than ^{99m}Tc-N4 in both cell lines. Biodistribution of ^{99m}Tc-N4-NIM showed increased tumor-to-blood and tumor-to-muscle count density ratios as a function of time. Oxygen tension in tumor tissue was 6–10 mmHg compared to 40–50 mmHg in normal muscle tissue. Planar imaging studies confirmed that the tumors could be visualized clearly with ^{99m}Tc-N4-NIM in animal models. Efficient synthesis of N4-NIM was achieved. ^{99m}Tc-N4-NIM is a novel hypoxic probe and may be useful in evaluating cancer therapy.

1. Introduction

Recent studies demonstrated that the hypoxic environment induces more malignant neoplastic phenotypes [1]. Disruption of oxygen delivery to tumors could diminish apoptotic potential and increase the chemotherapy/radiation resistance, while an improvement in oxygen delivery to tumors increases tumor sensitivity to radiation and chemotherapy [2–4]. Due to its significant prognostic and therapeutic implication, efforts have been made to invent efficient noninvasive methods to assess the presence and extent of tumor hypoxia because information on the hypoxic fraction in tumors could aid to reveal the mechanisms of aggressive behavior. The success of the endeavor to noninvasively detect the hypoxic fraction of tumor by nuclear molecular imaging such as single-photon emission computed tomography (SPECT) allows physicians to select patients for additional or alternative treatment regimens that may circumvent or overcome the ominous impact of tumor hypoxia and improve disease control [5].

The nitro group of nitroimidazole is enzymatically reduced by ribonucleoside reductase within viable hypoxic cells. This mechanism is well understood through numerous *in vitro* and *in vivo* studies from the past three decades [6]. In aerobic cells the reduced nitroimidazole is immediately reoxidized and washed out rapidly. On the contrary, in cells with low oxygen concentration the reoxidation is slowed, which allows further reductive reactions to take place. This leads to the formation of reactive products that could covalently bind to cell components and thus diffuse more slowly out of the tissue in an oxygen-dependent manner [7]. ^{18}F-Fluoromisonidazole (^{18}F-FMISO) and ^{18}F-fluoroerythronitroimidazole (^{18}F-FETNIM), 2-nitroimidazole analogues, have been used with PET to evaluate tumor

hypoxia, but the chemistries are dependent on a cyclotron to produce ^{18}F in addition to slow serum clearances [8–10].

In an attempt to identify efficient and clinically user-friendly chelator-based hypoxia tracers, our team has developed a new class of ^{99m}Tc hypoxia SPECT tracers based on the nitroimidazole backbone. The nitrogen, oxygen, and sulfur combination has shown to be stable chelators for radiometals [11–18]. The chelator used in this paper is 1,4,8,11-tetraazabicyclohexadecane (N4) which has shown to be a stable chelator for ^{99m}Tc [11, 12]. In addition, N4-chemistry could be easily modified and selectively reacted with halogenated homing compounds. In this paper, the potential use of ^{99m}Tc-N4-NIM as tumor hypoxic imaging agent was evaluated. The advantage of ^{99m}Tc-N4-nitroimidazole over ^{18}F-FMISO and ^{18}F-FETNIM is its easier chemistry and its water solubility that may lead to the rapid clearance of unbounded tracers after intravenous injection.

2. Materials and Methods

2.1. Chemicals and Analysis. All chemicals of analytical grade and solvents of high performance liquid chromatography (HPLC) grade were obtained from Sigma-Aldrich (St. Louis, MO, USA). Nuclear magnetic resonance (NMR) was performed on a Bruker 300-MHz spectrometer (Bruker BioSpin Corporation, Billerica, MA, USA), and mass spectra were performed on a Waters Q-TOF Ultima mass spectrometer (Waters, Milford, MA, USA) at the chemistry core facility at The University of Texas MD Anderson Cancer Center (Houston, TX, USA). Sodium pertechnetate ($Na\,^{99m}TcO_4$) was obtained from a $^{99}Mo/^{99m}Tc$ generator (Covidien, Mansfield, MA, USA).

2.2. Sodium Salt of 2-Nitroimidazole (Compound 1). The synthetic scheme of N4-NIM is shown in Figure 1. One molar equivalent of NaOH 1 M (0.3864 g, 9.66 mmol, 9.66 mL) was added to 2-nitroimidazole (1.09 g, 9.66 mmol) and warmed 30 minutes at 50°C to dissolve it. If the compound was not dissolved in the solution then NaOH was added drop by drop until the solid was dissolved completely and we continue heating for 15 minutes more. Water was removed on rotary evaporator. Crude compound was dissolved in minimum quantity of water, filtered, and lyophilized. Yield: 5.31 g, (90%).

2.3. Bromopropane Nitroimidazole (Compound 2). In two-neck flask one molar equivalent of Sodium salt of 2-nitroimidazole (2.00 g, 14.7 mmol) in solid form was added in 40 mL of acetonitrile (anhydrous) to dissolve it, then 18-crown-6 (3.88 g, 14.7 mmol) was added to this mixture. In nitrogen atmosphere 12.5 molar equivalent of 1,3-dibromopropane (18.65 mL, 183.76 mmol, 37.09 g) was added to the reaction mixture. The reaction mixture was then refluxed in a nitrogen environment at 50°C overnight. The reaction was filtered to purify the precipitate of NaBr using the 0.22 μM filter paper. Soon after the solvent was evaporated, the crude compound was purified by column chromatography with a $CHCl_3 : CH_3OH$ mixture (v : v, 9 : 1). Yield: 10.45 g (90%).

2.4. N^1, N^4-Dioxylyl-1,4,8,11-Tetraazacyclotetradecane (Compound 3). 1,4,8,11-Tetraazacyclotetradecance (N4) (2.997 g, 14.974 mmol) was dissolved in 50 mL of ethanol (anhydrous) ethanol, and after heating at 50°C, diethyl oxalate (2.188 g, 14.974 mmol, 2.03 mL) was added. The reaction mixture was refluxed for 18 hours at 75°C. The solvent was rotary evaporated and the crude product was dissolved in minimum quantity of ethanol and the turbid solution was filtered with 0.22 μM filter. Crude compound was dissolved in minimum amount of anhydrous ethanol and kept rotating on rotary evaporator for 40 minutes at 40–50°C. The compound was crystallized by adding 200 mL acetone (anhydrous) leaving the solution overnight in the refrigerator to yield white crystals of N^1, N^4-dioxylyl-1,4,8,11-tetraazacyclotetradecane. Yield: 8.64 g (52.04%) Ms (m/z) 255.19 $[M]^+$.

2.5. 1-[3-(2-Nitroimidazole-1-yl)propyl]-(N^1,N^4-Dioxylyl-1, 4,8,11-Tetraazacyclotetradecane) (Compound 4). N^1,N^4-dioxylyl-1,4,8,11-tetraazacyclotetradecane (0.5746 g, 2.259 mmol) was placed into the two-neck flask and dissolved in 25 mL of DMF (anhydrous). While heating the solution at 50°C, bromonitroimidazole (0.5329 g, 2.259 mmol) dissolved in 2.0 mL of DMF (anhydrous) was added to the reaction mixture. After adding K_2CO_3 (anhydrous) (0.7805 g; 5.6475 mmol) in 2.5 molar equivalent solid to the reaction mixture, it was refluxed at 70°C overnight. Crude compound was filtered using 0.22 μM filter paper and checked by TLC in chloroform: methanol in an 8 : 2 solvent system. Solvent was then evaporated and crude compound was purified by column chromatography in (8 : 2) of chloroform and methanol. Yield: 6.96 g, (75.86%). Ms (m/z) 408.30 $[M]^+$.

2.6. 1-[3-(2-Nitroimidazole-1-yl)propyl]-(1,4,8,11-Tetraazacyclotetradecane) (Compound 5, N4-NIM). To a 1 equivalent solution of (N4OxaNIM) N^1,N^4-dioxylyl-1,4,8,11-tetraazacyclotetradecane (0.100 g; 0.246 mmol) in 1 mL of water, 10 equivalents of 10 N NaOH (0.246 mL) were added, stirred, and refluxed over night at 75°C. The solvent was evaporated under vacuum, giving off white solid. The crude compound was dissolved in minimum quantity of water and filtered, then purified by sephadex G25 column. The fractions were lyophilized and collected by checking ^1H NMR as off white solid. Yield: 0.045 g (52.32%).

2.7. Radiolabeling of N4-NIM with ^{99m}Tc. Radiosynthesis of ^{99m}Tc-N4-NIM was achieved by adding a required amount of ^{99m}Tc-pertechnetate into a kit containing the lyophilized residue of N4-NIM (1 mg) and $SnCl_2$ (100 μg). Final pH of the preparation was 5.5–7.4. Radiochemical purity was determined by TLC and HPLC. Radio-TLC (Waterman No. 1) was obtained by eluting ^{99m}Tc-N4-NIM with acetone and saline, respectively. Radio-HPLC (Waters) was obtained by eluting ^{99m}Tc-N4-NIM on a C-18 reverse phase column (4.5 × 250 mm, 5 μm diameter, Zorbax Extend C 18, Agilant Technologies, Santa Clara, CA, USA) with 8 : 2 acetonitrile: water solution (v : v) using a flow rate of 0.5 mL/minute

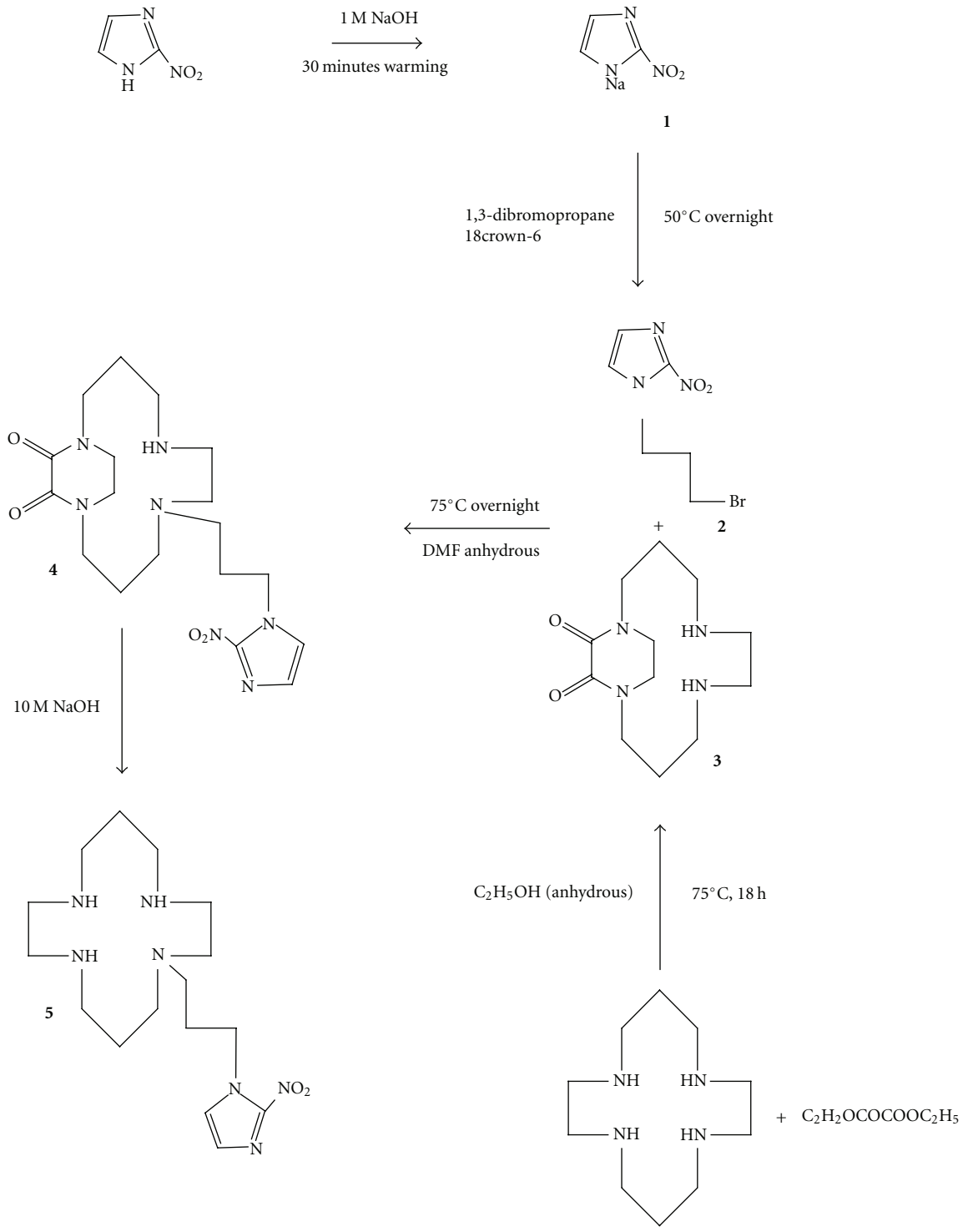

Figure 1: Synthetic scheme of N4-NIM.

at UV 210 and 254 nm. The concentration of ^{99m}Tc-N4-NIM was 1.0 mg/1.96 mCi/500 μL H_2O. The concentration of unlabeled N4-NIM was 1.7 mg/200 μL H_2O.

2.8. Cellular Uptake of ^{99m}Tc-N4-NIM. The 13762 mammary cancer cells and mesothelioma cells (IL-45) were plated to 6-well tissue culture plates that contained 2×10^5 cells/well and incubated with ^{99m}Tc-N4-NIM (0.05 mg/well, 8 μCi/well) and ^{99m}Tc-N4 (0.025 mg/well, 8 μCi/well) for 0–4 hours. After incubation, cells were washed with ice-cold phosphate-buffered solution twice and detached using a treatment of 0.5 mL of trypsin for 5 minutes. Cells were then collected and the radioactivity of the cells was measured in triplicate with a gamma counter. Radioactivity was expressed as mean ± standard deviation percent of cellular uptake (%Uptake).

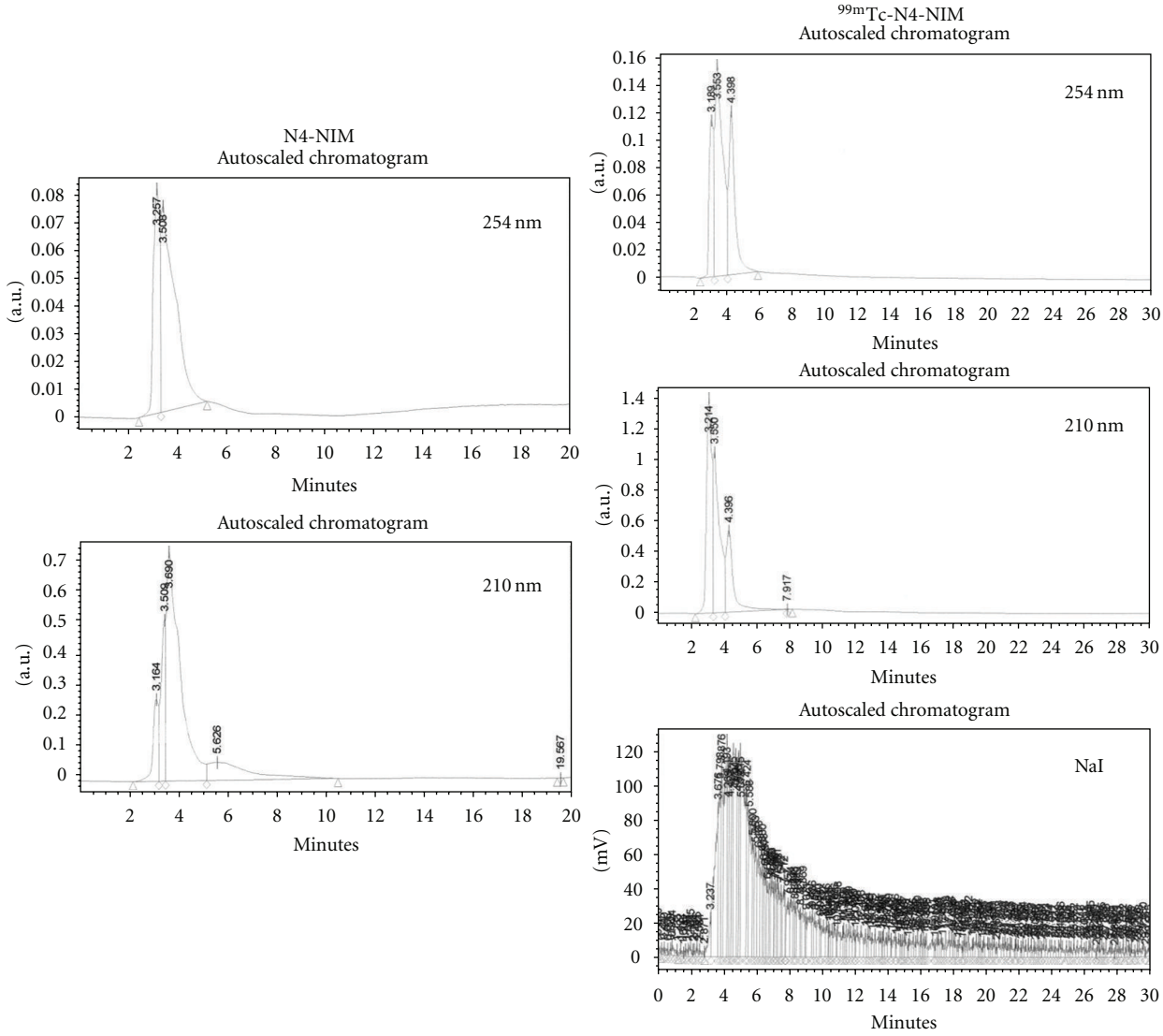

Figure 2: HPLC analysis of N4-NIM (left) and ^{99m}Tc-N4-NIM (right). The purity of both N4NIM and ^{99m}Tc-N4-NIM was 96%.

2.9. Biodistribution and Radiation Dosimetry Estimates of ^{99m}Tc-N4-NIM. The animal experiments were carried out in compliance with the relevant national laws relating to the conduct of animal experimentation. The animal protocol was approved by The University of Texas M. D. Anderson Cancer Center Animal Care and Use Committee (IACUC). Female Fischer 344 rats (150 ± 25 g) (Harlan Sprague-Dawley, Indianapolis, IN) were inoculated subcutaneously with 0.1 mL of mammary tumor cells from the 13762 tumor cell line suspension (10^6 cells/rat, a tumor cell line specific to Fischer rats) into the hind legs using 25-gauge needles. Studies were performed 14 to 17 days after implantation when tumors reached approximately 1 cm diameter. The rats were divided into 3 groups and each rat was injected intravenously with 25 ± 0.5 μCi of ^{99m}Tc-N4-NIM and ^{99m}Tc-N4. Each group was examined at 1 of 3 time points (0.5, 2, or 4 hours after injection). At each time point, the rats were killed and the selected tissues were excised, weighed, and measured for radioactivity by gamma counter. For each sample, radioactivity was expressed as mean percentage of the injected dose per gram of tissue wet weight (%ID/g). Counts from a 1/10 diluted sample of the original injection were used as a reference.

Tumor/nontarget tissue count density ratios were calculated from the corresponding %ID/g values. Olinda software (version 1.1; Vanderbilt University, Nashville, TN, USA) was used to determine dosimetry, based upon preclinical source organ residence time estimates as followed: rat organ distribution data was processed using in-house software to determine residence times (τ) based on AUC. The data was then converted to human residence time estimates using the correction factor for each organ, and subsequent τ values were entered into Olinda software to generate human dose estimates.

2.10. Polarographic pO_2 Measurements of Mammary Tumors. To confirm tumor hypoxia, intratumoral pO_2 measurements

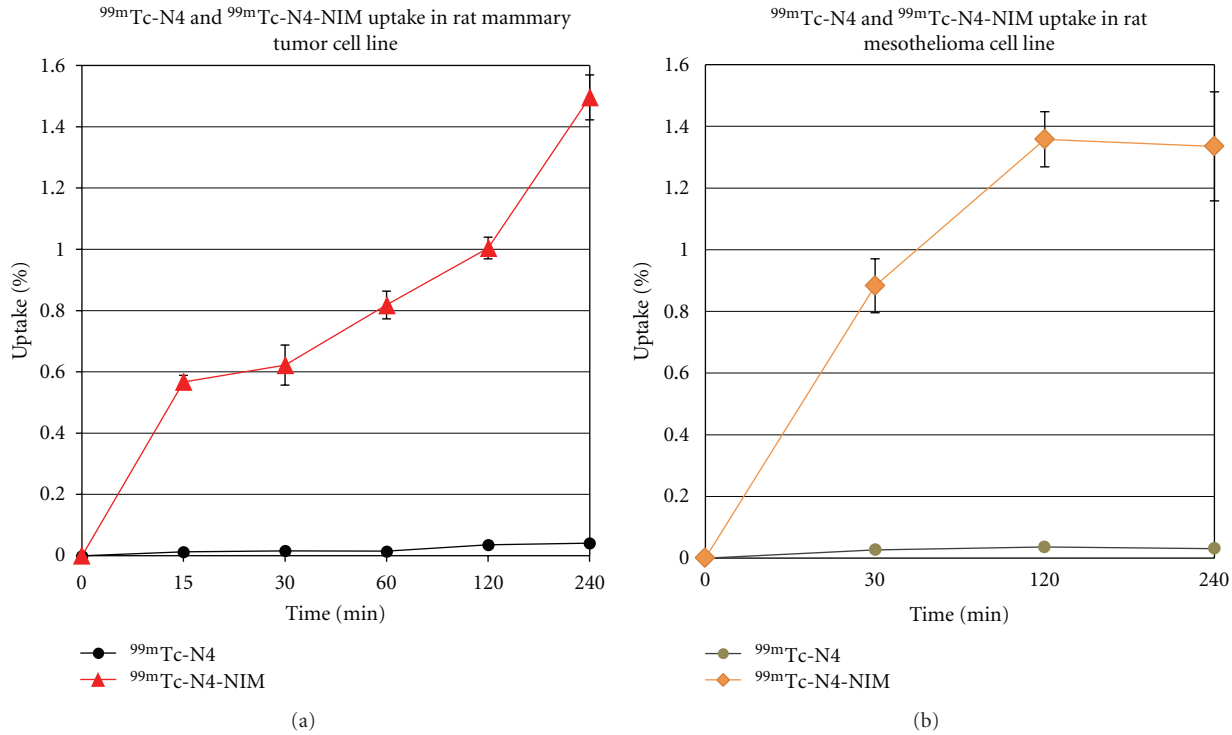

Figure 3: *In vitro* cell uptake studies using rat mammary cancer cells and mesothelioma cells revealed that ^{99m}Tc-N4-NIM had high uptake in both cell lines.

were performed using the Eppendorf computerized histographic system. Twenty to twenty-five pO_2 measurements along each of two to three linear tracks were performed at 0.4 mm intervals on each tumor (40–75 measurements total). Tumor pO_2 measurements were made on three tumor-bearing rats. Using an on-line computer system, the pO_2 measurements of each track were expressed as absolute values relative to the location of the measuring point along the track and as the relative frequencies within a pO_2 histogram between 0 and 100 mmHg with a class width of 2.5 mm.

2.11. Planar Scintigraphic Imaging in Tumor-Bearing Models. Two animal models were created. For Rabbit model, the VX-2 tumor mass was inoculated (im) to the thigh region of male New Zealand white rabbits (2 kg). For rat model, cells from the mammary tumor cell line 13762, suspended in phosphate-buffered solution (10^5 cells/0.1 mL solution per rat), were injected subcutaneously into the right calf muscle of female Fischer 344 rats. Planar scintigraphic imaging of ^{99m}Tc-N4-NIM was performed 12–14 days after inoculation when tumors reached approximately 1 cm in diameter. The animals were anesthetized and injected intravenously with ^{99m}Tc-N4-NIM (0.3 mg/rat, 300 μCi/rat; 1.5 mCi/rabbit), and images were acquired at 30, 120, and 240 minutes after administration of tracers. Planar scintigraphic images were obtained using M-CAM (Siemens Medical Solutions, Hoffman Estates, IL, USA) equipped with a low-energy high-resolution collimator. Computer-outlined regions of interest (ROIs in counts per pixel) between tumor and muscle tissue were used to calculate tumor-to-muscle (T/M) ratios. Percent of injected dose (%ID) in the tumor was also calculated from the reference standard, which was 1/10 of the original injection activity of ^{99m}Tc-N4-NIM.

3. Results

3.1. Chemistry and Radiochemistry. The synthetic scheme is shown in Figure 1. The total synthesis yield of precursor N4-NIM via our 5-step procedure was 14%. The structure and purity of N4-NIM were confirmed by ^{1}H- and ^{13}C-NMR, mass spectra, and HPLC. The N4-NIM ^{1}H-NMR results (D_2O δ, ppm) were as follows: 8.25 (s, H, imidazole ring), 3.74 (s, H, imidazole ring), 3.17–3.25 (t, 2H,CH_2 of propyl group), 3.05–2.91 (t, 2H, CH_2 of propyl group), 2.26–2.76 (m, 2H, CH_2 of propyl group), 2.28–2.48 (m, 14H, CH_2 of N4 ring), and 1.38–1.68 (m, 6H, CH_2 of N4 ring). ^{13}C-NMR results (D_2O δ, ppm) were as follows: 180.27, 173.13, 164.13, 61.48, 54.13, 51.73, 50.20, 49.45, 48.29, 46.61, 24.64, 23.76, and 22.64. Ms (m/z) 377.24 $[M]^+$. In radio-TLC analysis, ^{99m}Tc-N4-NIM did not migrate either in saline or acetone solvent. HPLC analysis showed that the retention time for N4-NIM was 3.506 min and 3.690 min at UV-254 and 210 nm, respectively. N4-NIM was labeled with ^{99m}Tc successfully with high radiochemical purity (>96%) (Figure 2). HPLC analysis showed the retention time for ^{99m}Tc-N4-NIM was 3.663 min (UV-254 nm), 3.650 min (UV-210 nm), and 4.200 min (NaI detector). Because ^{99m}Tc-N4-NIM is a kit product and labeled without any further purification, its radiochemical yield was assumed to be identical to its radio-chemical purity.

Table 1: Biodistribution of ^{99m}Tc-N4 in mammary tumor-bearing rats.

	% of injected dose per gram of tissue weight (n = 3/time, interval, iv)		
	30 min	120 min	240 min
Blood	0.23 ± 0.009	0.04 ± 0.002	0.02 ± 0.002
Heart	0.07 ± 0.005	0.01 ± 0.001	0.01 ± 0.000
Lung	0.20 ± 0.011	0.05 ± 0.002	0.03 ± 0.001
Thyroid	0.25 ± 0.011	0.03 ± 0.002	0.02 ± 0.001
Pancreas	0.07 ± 0.007	0.02 ± 0.002	0.02 ± 0.001
Liver	2.98 ± 0.083	1.14 ± 0.018	0.79 ± 0.026
Spleen	0.35 ± 0.026	0.37 ± 0.007	0.39 ± 0.020
Kidney	2.56 ± 0.101	1.11 ± 0.045	0.65 ± 0.028
Stomach	0.12 ± 0.005	0.02 ± 0.001	0.01 ± 0.000
Intestine	0.25 ± 0.004	0.39 ± 0.048	0.14 ± 0.003
Uterus	0.16 ± 0.014	0.02 ± 0.001	0.01 ± 0.001
Tumor	0.09 ± 0.004	0.03 ± 0.003	0.02 ± 0.001
Muscle	0.05 ± 0.002	0.01 ± 0.000	0.01 ± 0.000
Bone	0.07 ± 0.001	0.02 ± 0.001	0.01 ± 0.000
Brain	0.01 ± 0.000	0.00 ± 0.000	0.00 ± 0.000
Tumor/blood	0.40 ± 0.002	0.78 ± 0.044	0.70 ± 0.008
Tumor/muscle	1.96 ± 0.015	5.32 ± 0.402	3.35 ± 0.147
Tumor/brain	6.19 ± 0.365	11.06 ± 0.667	11.93 ± 0.675

Value shown represents the mean ± standard deviation of data from 3 animals.

3.2. In Vitro Cellular Uptake Assays. The cellular uptake kinetics of ^{99m}Tc-N4-NIM and ^{99m}Tc-N4 in rat mammary tumor cells and rat mesothelioma cells are shown in Figure 3. The uptake for ^{99m}Tc-N4-NIM increased dramatically up to 240 minutes, but this was not the case for the ^{99m}Tc-N4, suggesting that ^{99m}Tc-N4-NIM can enter tumor cells specifically and accumulate rapidly.

3.3. Biodistribution and Radiation Dosimetry Estimates of ^{99m}Tc-N4-NIM. Tissue distribution of ^{99m}Tc-N4 and ^{99m}Tc-N4-NIM is shown in Tables 1 and 2. Biodistribution studies showed that tumor/blood and tumor/muscle count density ratios at 0.5–4 hr gradually increased for ^{99m}Tc-N4-NIM (Table 2). No significant uptake in thyroid and stomach suggests *in vivo* stability of ^{99m}Tc-N4-NIM. The optimal tumor imaging time for ^{99m}Tc-N4-NIM is at 2 hr post-administration of ^{99m}Tc-N4-NIM. Although tumor/blood and tumor/muscle count density ratios at 0.5–4 hr gradually increased for ^{99m}Tc-N4, yet there was almost no tumor uptake (Table 1). Based upon preclinical studies, dosimetry of ^{99m}Tc-N4-NIM was estimated from MIRDose. It is safe to use ^{99m}Tc-N4-NIM in human because the whole body, liver, and effective dose equivalent for the proposed single dose at 20 mCi of ^{99m}Tc-N4-NIM were less than the limits for 3 rem annual and 5 rem total dose equivalent, and other organs of single dose at 5 rem annual and total dose equivalent at 15 rem if the subject did not have any other radiation exposure (Table 3).

Table 2: Biodistribution of ^{99m}Tc-N_4-NIM in mammary tumor-bearing rats.

	% of injected dose per gram of tissue weight (n = 3/time, interval, iv)		
	30 min	2 h	4 h
Blood	0.76 ± 0.06	0.20 ± 0.01	0.16 ± 0.01
Heart	0.26 ± 0.03	0.07 ± 0.01	0.04 ± 0.00
Lung	0.58 ± 0.06	0.17 ± 0.00	0.10 ± 0.00
Thyroid	0.71 ± 0.06	0.17 ± 0.01	0.08 ± 0.00
Pancreas	0.22 ± 0.03	0.06 ± 0.00	0.04 ± 0.01
Liver	0.88 ± 0.05	0.84 ± 0.03	0.51 ± 0.02
Spleen	0.74 ± 0.13	0.42 ± 0.01	0.70 ± 0.02
Kidney	4.92 ± 0.89	4.42 ± 0.06	1.33 ± 0.10
Stomach	0.37 ± 0.04	0.09 ± 0.01	0.03 ± 0.00
Intestine	0.33 ± 0.04	0.15 ± 0.07	0.04 ± 0.01
Uterus	0.61 ± 0.16	0.20 ± 0.11	0.08 ± 0.01
Tumor	0.52 ± 0.02	0.20 ± 0.00	0.08 ± 0.00
Muscle	0.18 ± 0.01	0.04 ± 0.00	0.02 ± 0.00
Bone	0.22 ± 0.08	0.14 ± 0.02	0.03 ± 0.00
Brain	0.04 ± 0.00	0.01 ± 0.00	0.01 ± 0.00
Tumor/blood	0.69 ± 0.02	1.01 ± 0.05	0.98 ± 0.06
Tumor/muscle	2.86 ± 0.19	5.69 ± 0.40	4.88 ± 0.56
Tumor/brain	12.74 ± 2.26	15.51 ± 2.16	15.10 ± 2.47

Values shown represent the mean ± standard deviation of data from 3 animals.

Table 3: Radiation dose estimates for the reference adult for ^{99m}Tc-N4-NIM.

Target organ	rad/mCi	Human dose (mCi)	rad
Organs (5 rem annual/15 rem total)			
Adrenals	$6.56E-03$	20	0.131
Brain	$5.03E-04$	20	0.010
Breasts	$1.22E-03$	20	0.024
Gall bladder wall	$4.28E-03$	20	0.086
Lli wall	$1.53E-03$	20	0.031
Small int	$2.97E-03$	20	0.059
Stomach	$4.19E-03$	20	0.084
Uli wall	$2.74E-03$	20	0.055
Heart wall	$5.50E-03$	20	0.110
Kidneys	$8.20E-02$	20	1.640
Liver	$4.41E-03$	20	0.088
Lungs	$5.05E-03$	20	0.101
Muscle	$1.46E-03$	20	0.029
Pancreas	$8.44E-03$	20	0.169
Bone surfaces	$4.11E-03$	20	0.082
Skin	$8.81E-04$	20	0.018
Testes	$8.11E-04$	20	0.016
Thymus	$1.69E-03$	20	0.034
Thyroid	$9.93E-04$	20	0.020
Urine bladder wall	$1.18E-03$	20	0.024
Uterus	$1.65E-03$	20	0.033
Eff dose	$3.41E-03$	20	0.068
Blood-forming organs (3 rem annual/5 rem total)			
Ovaries	$1.67E-03$	20	0.033
Red marrow	$2.15E-03$	20	0.043
Spleen	$3.27E-02$	20	0.654
Eff dose eq	$9.73E-03$	20	0.195
Total body	$2.26E-03$	20	0.045

3.4. Polarographic Oxygen Microelectrode pO_2 Measurements. Intratumoral pO_2 measurements of mammary tumors indicated the tumor oxygen tension ranged 4.6 ± 1.4 mmHg as compared to normal muscle of 35 ± 10 mmHg. The data indicated that the tumors were hypoxic.

3.5. Planar Scintigraphic Imaging in Tumor-Bearing Models. The selected planar scintigraphic images of tumor-bearing rats and rabbits after ^{99m}Tc-N4-NIM injection are shown in Figures 4 and 5. Tumors could be clearly detected by ^{99m}Tc-N4-NIM. The T/M ratios at 60–120 minutes were 4.1–4.2 in tumor-bearing rats and 2.52–2.98 in tumor-bearing rabbits, respectively.

4. Discussion

The development of new tumor hypoxia agents is clinically desirable for detecting primary and metastatic lesions as well as predicting radioresponsiveness and time to recurrence [10, 19]. None of the contemporary imaging modalities accurately measures hypoxia since the diagnosis of tumor hypoxia requires a pathologic examination. It is often difficult to predict the outcome of a therapy for hypoxic tumor without knowing at least the baseline of hypoxia in each tumor treated. Although the Eppendorf polarographic oxygen microelectrode can measure the oxygen tension in a tumor, this technique is invasive and needs a skillful operator. Additionally, this technique can only be used on accessible tumors (e.g., head and neck, cervical) and multiple readings are needed. Therefore, an accurate and easy method of measuring tumor hypoxia will be useful for patient selection. However, tumor-to-normal tissue uptake ratios vary and depend upon the radiopharmaceuticals used. Therefore, it would be rational to correlate tumor-to-normal tissue uptake ratios with the gold standard Eppendorf electrode measures of hypoxia when new radiopharmaceuticals are introduced to clinical practice.

In biodistribution, ^{99m}Tc-N4-NIM in tumor tissue was decreased as same as ^{99m}Tc-N4 (Tables 1 and 2). This decreased uptake might be due to slower uptake ^{99m}Tc-N4 and ^{99m}Tc-N4-NIM as a function of increased renal excretion. However, the tumor uptake as well as tumor/blood and tumor/muscle ratios in ^{99m}Tc-N4-NIM were higher than that in ^{99m}Tc-N4 group.

Hypoxia-Inducible Factor (HIF)-1α/β heterodimer is a master transcription factor for several genes involved in angiogenesis, glycolysis, pH balance, and metastasis. These HIF-1 target genes help tumors to overcome forthcoming metabolic obstacles as they grow. Under normoxic condition, the HIF-1α subunit is hydroxylated by its specific prolyl-4 hydroxylase 2, given the acronym PHD2, thus stabilizing it under normoxic conditions [20]. *In vitro* cellular uptake assay, the uptake of ^{99m}Tc-N4-NIM in tumor cells increases up to 240 min. However, this assay was performed under normoxic condition. The increased uptake of ^{99m}Tc-N4-NIM in tumor cells under normoxic condition might be due to stabilized HIF-1α. $NaTcO_4$ was reduced to $^{+5}$Tc [O] and bound to the three nitrogens of cyclam. The charge of ^{99m}Tc-N4-NIM is neutral. Cell uptake of ^{99m}Tc-N4-NIM was via passive diffusion.

In our animal model, tumor oxygen tension was determined to be 3.2 to 6.0 mmHg, whereas normal muscle tissue had 30 to 40 mmHg. Although another factor such as anemia may have influenced the level of tumor hypoxia, there was no attempt in identifying this factor. In biodistribution, ^{99m}Tc-N4-NIM in tumor tissue was decreased as same as ^{99m}Tc-N4 (Tables 1 and 2). This decreased uptake might be due to slower uptake of ^{99m}Tc-N4 and ^{99m}Tc-N4-NIM as a function of increased renal excretion. However, the tumor uptake as well as tumor/blood and tumor/muscle ratios in ^{99m}Tc-N4-NIM was higher than those in ^{99m}Tc-N4 group.

Due to better imaging characteristics and lower cost, attempts are made to replace the ^{123}I-, ^{131}I-, ^{67}Ga-, and ^{111}In-labeled compounds with corresponding ^{99m}Tc-labeled compounds when possible. Our radiochemistry data indicated N4-NIM could be labeled with ^{99m}Tc very easily and efficiently at room temperature with high radiochemical purity.

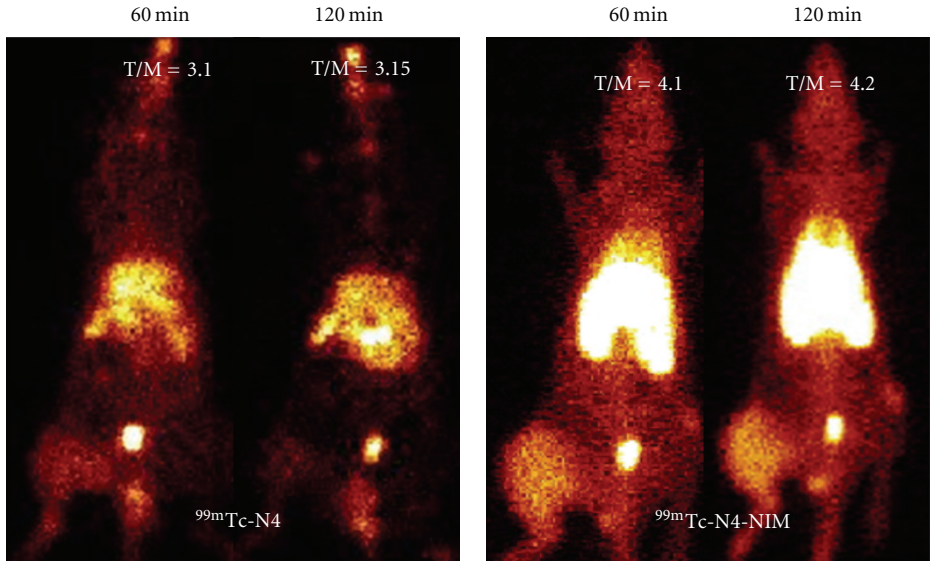

Figure 4: Planar scintigraphy of ^{99m}Tc-N4 and ^{99m}Tc-N4-NIM (400 μCi/rat, iv, acquired 500,000 count) showed higher tumor-to-muscle count density ratio in ^{99m}Tc-N4-NIM compared to that of ^{99m}Tc-N4. The numbers are tumor-to-muscle count density ratios (counts/pixel) at 60–120 min.

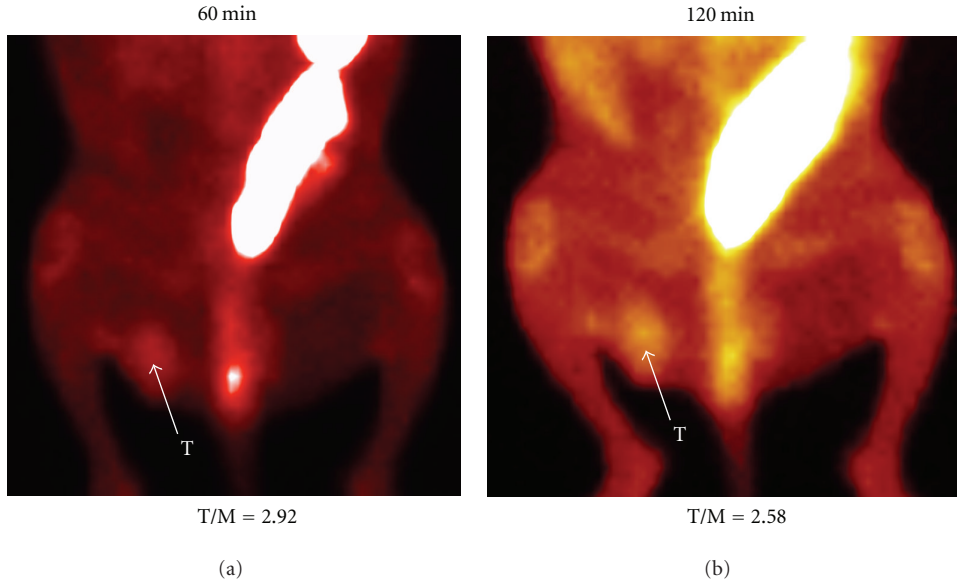

Figure 5: Planar scintigraphy of ^{99m}Tc-N4-NIM (15 mCi/rabbit, iv, acquired 500,000 count) showed higher tumor-to-muscle count density ratio (counts/pixel) at 60 and 120 min.

In vivo tissue distribution studies showed that radiation dosimetry of blood-forming organs was within radiation dose limits. Our planar imaging studies indicate that ^{99m}Tc-N4-NIM is feasible to assess tumor hypoxia.

In summary, N4-NIM kits could be labeled with ^{99m}Tc easily and efficiently, with high radiochemical purity and cost-effectiveness. *In vitro* cellular uptake and scintigraphic imaging studies demonstrated the pharmacokinetic distribution and feasibility of using ^{99m}Tc-N4-NIM for tumor hypoxia imaging.

Acknowledgments

This work was supported in part by a Sponsored Research Grant (MDA LS2005-00012803PL) established between

MDACC and Cell>Point L.L.C. and the J. S. Dunn Foundation. The chemistry analysis and animal research are supported by M. D. Anderson Cancer Center (CORE) Grant NIH CA-16672.

References

[1] B. C. Liang, "Effects of hypoxia on drug resistance phenotype and genotype in human glioma cell lines," *Journal of Neuro-Oncology*, vol. 29, no. 2, pp. 149–155, 1996.

[2] A. J. Giaccia, "Hypoxic stress proteins: survival of the fittest," *Seminars in Radiation Oncology*, vol. 6, no. 1, pp. 46–58, 1996.

[3] T. G. Graeber, C. Osmanian, T. Jacks et al., "Hypoxia-mediated selection of cells with diminished apoptotic potential in solid tumours," *Nature*, vol. 379, no. 6560, pp. 88–91, 1996.

[4] S. Dai, M. L. Huang, C. Y. Hsu, and K. S. C. Chao, "Inhibition of hypoxia inducible factor 1α causes oxygen-independent cytotoxicity and induces p53 independent apoptosis in glioblastoma cells," *International Journal of Radiation Oncology Biology Physics*, vol. 55, no. 4, pp. 1027–1036, 2003.

[5] J. M. Brown, "The hypoxic cell: a target for selective cancer therapy—eighteenth Bruce F. Cain Memorial Award Lecture," *Cancer Research*, vol. 59, no. 23, pp. 5863–5870, 1999.

[6] T. Chu, R. Li, S. Hu, X. Liu, and X. Wang, "Preparation and biodistribution of technetium-99m-labeled 1-(2-nitroimidazole-1-yl)-propanhydroxyiminoamide (N2IPA) as a tumor hypoxia marker," *Nuclear Medicine and Biology*, vol. 31, no. 2, pp. 199–203, 2004.

[7] B. M. Seddon, R. J. Maxwell, D. J. Honess et al., "Validation of the fluorinated 2-nitroimidazole SR-4554 as a non-invasive hypoxia marker detected by magnetic resonance spectroscopy," *Clinical Cancer Research*, vol. 8, no. 7, pp. 2323–2335, 2002.

[8] L. Bentzen, S. Keiding, M. Nordsmark et al., "Tumour oxygenation assessed by 18F-fluoromisonidazole PET and polarographic needle electrodes in human soft tissue tumours," *Radiotherapy and Oncology*, vol. 67, no. 3, pp. 339–344, 2003.

[9] T. Grönroos, L. Bentzen, P. Marjamäki et al., "Comparison of the biodistribution of two hypoxia markers [18F]FETNIM and [18F]FMISO in an experimental mammary carcinoma," *European Journal of Nuclear Medicine and Molecular Imaging*, vol. 31, no. 4, pp. 513–520, 2004.

[10] M. B. Mallia, S. Subramanian, A. Mathur, H. D. Sarma, M. Venkatesh, and S. Banerjee, "Comparing hypoxia-targeting potential of 99mTc(CO) 3-labeled 2-nitro and 4-nitroimidazole," *Journal of Labelled Compounds and Radiopharmaceuticals*, vol. 51, no. 8, pp. 308–313, 2008.

[11] K. M. Herzog, E. Deutsch, K. Deutsch, E. B. Silberstein, R. Sarangarajan, and W. Cacini, "Synthesis and renal excretion of technetium-99m-labeled organic cations," *Journal of Nuclear Medicine*, vol. 33, no. 12, pp. 2190–2195, 1992.

[12] F. L. Kong, M. S. Ali, Y. Zhang et al., "Synthesis and evaluation of amino acid-based radiotracer ^{99m}Tc-N4-AMT for breast cancer imaging," *Journal of Biomedicine and Biotechnology*, vol. 2011, Article ID 276907, 7 pages, 2011.

[13] S. Liu, "The role of coordination chemistry in the development of target-specific radiopharmaceuticals," *Chemical Society Reviews*, vol. 33, no. 7, pp. 445–461, 2004.

[14] S. Liu, "Bifunctional coupling agents for radiolabeling of biomolecules and target-specific delivery of metallic radionuclides," *Advanced Drug Delivery Reviews*, vol. 60, no. 12, pp. 1347–1370, 2008.

[15] K. Ohtsuki, K. Akashi, Y. Aoka et al., "Technetium-99m HYNIC-annexin V: a potential radiopharmaceutical for the in-vivo detection of apoptosis," *European Journal of Nuclear Medicine*, vol. 26, no. 10, pp. 1251–1258, 1999.

[16] C. G. Van Nerom, G. M. Bormans, M. J. De Roo, and A. M. Verbruggen, "First experience in healthy volunteers with technetium-99m L,L-ethylenedicysteine, a new renal imaging agent," *European Journal of Nuclear Medicine*, vol. 20, no. 9, pp. 738–746, 1993.

[17] C. H. Kao, S. P. ChangLai, P. U. Chieng, and T. C. Yen, "Technicium-99m methoxyisobutylisonitrile chest imaging of a small cell lung carcinoma: relation to patient prognosis and chemotherapy response- a preliminary report," *Cancer*, vol. 83, pp. 64–68, 1998.

[18] H. C. Wu, C. H. Chang, M. M. Lai, C. C. Lin, C. C. Lee, and A. Kao, "Using Tc-99m DMSA renal cortex scan to detect renal damage in women with type 2 diabetes," *Journal of Diabetes and Its Complications*, vol. 17, no. 5, pp. 297–300, 2003.

[19] J. M. Brown and A. J. Giaccia, "The unique physiology of solid tumors: opportunities (and problems) for cancer therapy," *Cancer Research*, vol. 58, no. 7, pp. 1408–1416, 1998.

[20] H. Y. Lee, T. Lee, N. Lee et al., "Src activates HIF-1α not through direct phosphorylation of HIF-1α-specific prolyl-4 hydroxylase 2 but through activation of the NADPH oxidase/Rac pathway," *Carcinogenesis*, vol. 32, no. 5, pp. 703–712, 2011.